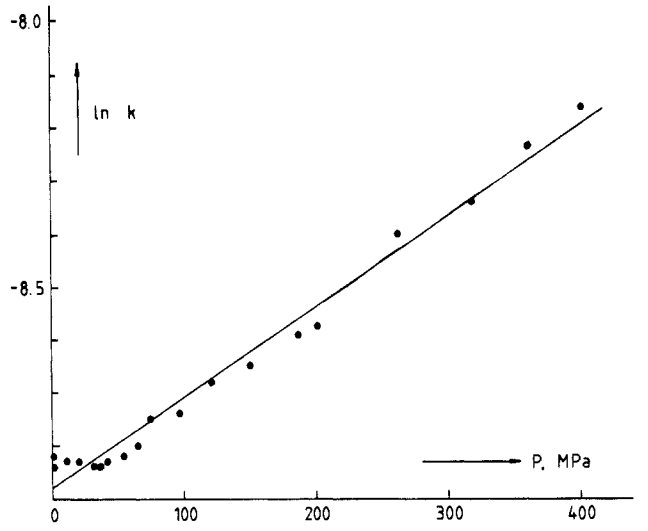

Figure 1. Pseudo-first-order rate constants as a function of pressure (1 MPa = 10 bar) for the hydrolysis of 2,4-dinitrophenyl phosphate at pH 12 (43.2 °C).

phosphonate to a substituted pyridine was found to be kinetically second-order and furthermore the second-order rate constants were not quite independent of the pK_a of the attacking pyridine.

Although a long-lived free intermediate is thus ruled out, there is at present no convincing proof for or against the fleeting existence of a metaphosphate ion which remains paired with the leaving group until it is captured. Even investigators who observed a metaphosphate transfer between polymer moieties were unable to give assurance that the reaction occurred without the intervention of a carrier.[9]

The volume change on going from a reactant to an intermediate is informative with regards to the competition between bond making and bond breaking processes.[10] The former is obviously associated with shrinkage and the latter with expansion. Typically the magnitudes of these changes may amount to 20 cm^3/mol (these values are calculated from the effect of hydrostatic pressure on the rates). For S_N2 displacement reactions in water both features contribute, but bond formation always dominates leading to activation volumes of −5 to −10 cm^3/mol. The expansions deduced from pressure-induced rate retardations have generally exceeded +10 cm^3/mol; for instance, the formation of CCl_2 in the base-promoted hydrolysis of chloroform has a $\Delta V^{\ddagger}$ of +16 cm^3/mol.

In view of these effects we felt an investigation of the rate of hydrolysis of 2,4-dinitrophenyl phosphate dianion as a function of pressure would yield information on the mechanisms of these reactions. This compound has been extensively investigated and these studies have produced evidence which supports[4,11] and disfavors[7a,b] a metaphosphate ion intermediate. The liberation of 2,4-dinitrophenoxide from the phosphate dianion was found to be accelerated by pressure (Figure 1) with $\Delta V^{\ddagger} = -4.8$ cm^3/mol. There is no way to reconcile this result with a free metaphosphate ion since simple bond cleavage should in this case have led to substantial charge delocalization which would have further magnified the expansion normally expected. The curvature often seen in such plots may screen the incursion of a small contribution from a second mechanism, however, there will then be a curvature in the Arrhenius plot. An examination of the temperature dependence of the rate, as shown in Figure 2, yielded a plot that was accurately linear over the whole range. This essentially rules out a significant contribution from a second mechanism.

We conclude that this reaction occurs by a nucleophilic attack by water at the phosphorus with loss of phenoxide ion. We must point out emphatically that these experiments have no bearing

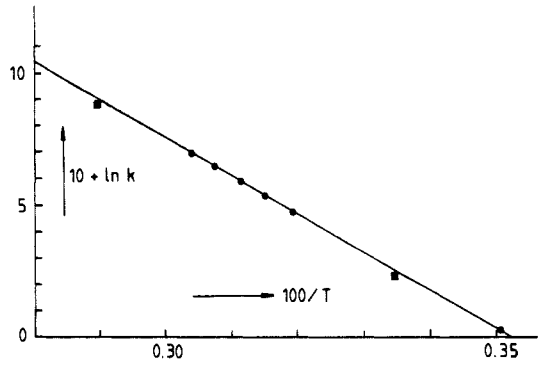

Figure 2. Arrhenius plot for the hydrolysis at atmospheric pressure. Square symbols represent data from the literature.[4a]

on the mechanism of the reaction in aprotic media.[12] The ion pairing that inevitably accompanies the use of nonaqueous solutions makes it impossible to depend on similar evidence in these media. Since the metaphosphate ion clearly has an independent existence in the gas phase but presumably not in water, there may be liquid media of intermediate internal pressure and/or nucleophilicity in which it may survive however briefly.

Acknowledgment. This work was supported by grants from the National Institutes of Health (HL 23126 to F.R.) and the National Science Foundation (W. le N.). W. le Noble also thanks the Humboldt Foundation for a Senior Fellowship at the University of Frankfurt where this manuscript was written. We thank Frau Baumgaertner who kindly drew the figures.

Supplementary Material Available: Rate data as a function of pressure and temperature (2 pages). Ordering information is given on any current masthead page.

(9) Rebek, J.; Gavina, F.; Navarro, C. *J. Am. Chem. Soc.* **1978**, *100*, 8113.
(10) le Noble, W. J.; Kelm, H.. *Angew Chem., Int. Ed. Engl.* **1980**, *19*, 841.
(11) (a) Gorenstein, D. G. *J. Am. Chem. Soc.* **1972**, *94*, 2523. (b) Gorenstein, D. G.; Lee, Y.-G.; Ker, D. *J. Am. Chem. Soc.* **1977**, *99*, 2264.

(12) Indeed, subsequent to the submission of this paper, evidence was published providing strong stereochemical support for a dissociative mechanism for the reaction of phenyl phosphate with *tert*-butyl alcohol in acetonitrile (Friedman, J. M.; Knowles, J. R. *J. Am. Chem. Soc.* **1985**, *107*, 6126). Further support for this mechanism was also reported for a P^1,P^1-disubstituted pyrophosphate in dichloromethane (Cullis, P. M.; Rous, A. J. *J. Am. Chem. Soc.* **1985**, *107*, 6721).

Evidence for the Formation of a $CoFe_3S_4$ Cluster in *Desulfovibrio gigas* Ferredoxin II

Isabel Moura and José J. G. Moura

Centro de Quimica Estrutural, UNL
1000 Lisboa, Portugal

Eckard Münck* and Vasilios Papaefthymiou

Gray Freshwater Biological Institute, University of Minnesota, Navarre, Minnesota 55392

Jean LeGall

Center for Biological Resource Recovery
Department of Biochemistry, University of Georgia
Athens, Georgia 30602

Received August 30, 1985

Using EPR and Mössbauer spectroscopy we have shown previously[1] that *Desulfovibrio gigas* ferredoxin II (Fd II) contains a 3Fe cluster. EXAFS studies[2] and chemical analyses[3] have suggested that this cluster has a cubane Fe_3S_4 core stoichiometry.

(1) Huynh, B. H.; Moura, J. J. G.; Moura, I.; Kent, T. A.; LeGall, J.; Xavier, A. V.; Münck, E. *J. Biol. Chem.* **1980**, *255*, 3242-3244.
(2) Antonio, M. R.; Averill, B. A.; Moura, I.; Moura, J. J. G.; Orme-Johnson, W. H.; Teo, B.-K.; and Xavier, A. V. *J. Biol. Chem.* **1982**, *257*, 6646-6649.
(3) Beinert, H.; Emptage, M. H.; Dreyer, J.-L.; Scott, R. A.; Hahn, J. E.; Hodgson, K. O.; Thomson, A. J. *Proc. Natl. Acad. Sci. U.S.A.* **1983**, *80*, 393-396.

0002-7863/86/1508-0349$01.50/0

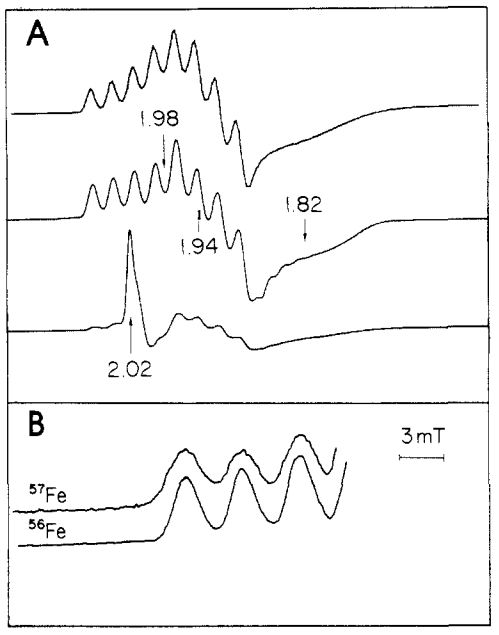

Figure 1. X-band EPR spectra of the oxidized CoFe cluster. (A) Middle trace: ^{56}Fe; T = 40 K; microwave power 1 mW; modulation amplitude, 0.5 mT. Lower trace: same as middle trace but T = 9 K. Upper trace: spectral simulation of 40 K spectrum using parameters quoted in the text. (B) Expanded view of low-field portion of 40 K spectra using samples containing ^{56}Fe (I = 0) and ^{57}Fe (I = $^1/_2$).

We have also shown[4] that the 3Fe cluster can be converted into a structure with a cubane Fe_4S_4 core. This conversion occurs with facility upon incubation of the protein with excess Fe^{2+} in the presence of dithiothreitol. Similar conversions have been reported for aconitase.[5] The facility of the $Fe_3S_4 \rightarrow Fe_4S_4$ conversions has suggested to us that one may be able to incorporate other metals into the vacant sites of a Fe_3S_4 cluster and thus generate a series of novel clusters. We report here evidence for the formation of a structure with a cubane $CoFe_3S_4$ core.

Fe II was purified and then incubated with excess metal similarly to the procedure described.[4] Typically 0.5 mL of dithionite-reduced Fd II, 0.5 mM in Fe_3S_4, was anaerobically incubated for 6–12 h with 15 mM $Co(NO_3)_2$ and 5 mM dithiothreitol and then repurified as described.[4] Addition of sulfide was not required. Metal analysis of four samples by plasma emission spectroscopy yielded, after correction for unconverted Fe_3S_4, (3 ± 0.3) Fe/Co. We call aerobically purified material the *oxidized* Co–Fe sample; this material is EPR-active. Upon addition of dithionite a *reduced*, EPR-silent, state was obtained.

Figure 1A (middle trace) shows an EPR spectrum of an oxidized sample. The spectrum exhibits eight well-resolved ^{59}Co (I = $^7/_2$) hyperfine lines centered around g_z = 1.98. The high-field portion of the g_z resonance is superimposed on a derivative-type feature at $g_y \approx 1.94$; the third principal resonance is centered at $g_x \approx 1.82$. Thus the spectrum of our *oxidized* sample is similar to the "g = 1.94" signals of *reduced* ($[Fe_4S_4]^+$) clusters. A spectral simulation (upper trace of Figure 1A) yielded $g_x \approx 1.82$, $g_y \approx 1.94$, g_z = 1.98 $A_x \approx A_y \approx 0$ mT, A_z = 4.4 mT, and line widths of 20, 15, and 2 mT along x, y, and z, respectively. A_x and A_y are quite uncertain because these parameters are strongly correlated with the widths along x and y.

In Figure 1B we show in an expanded view the first three low-field resonances for samples containing ^{56}Fe (lower trace) and ^{57}Fe (upper trace). The observation of line broadening of 0.6 mT by ^{57}Fe of the "^{59}Co hyperfine resonances" demonstrates that the EPR signal results from a cluster containing both Co and Fe, suggesting the Co has been incorporated into the vacant site of the Fe_3S_4 cluster. The observations of EPR signals around g = 2 suggests that the system has a spin S = $^1/_2$. Quantitation of the 40 K EPR signal against a copper perchlorate standard gave repeatedly ≈1 spin/Co. We have observed no other EPR-active species in either oxidized or reduced material, suggesting that the samples are free of adventitiously bound Co(II).

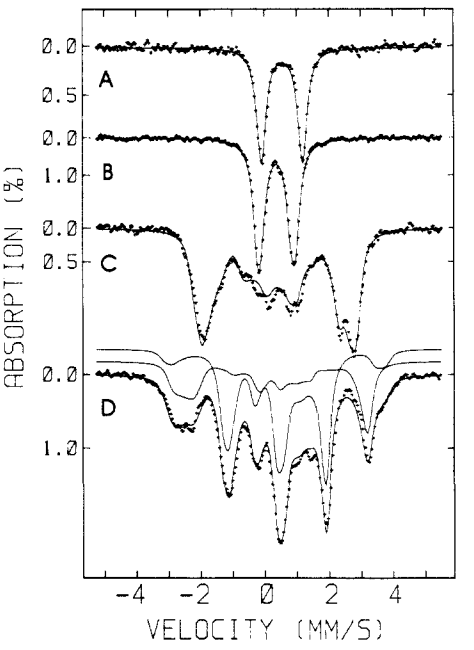

Figure 2. Mössbauer spectra of reduced (A) and oxidized (B–D) CoFe cluster. (A) Dithionite reduced sample at 4.2 K in zero applied field; (B) oxidized sample at T = 183 K; (C and D) oxidized sample at 4.2 K in 60 mT and 6.0 T parallel fields, respectively. Solid lines in (C) and (D) are computer simulations with parameters of Table I. Theoretical spectra of subsites I (two Fe atoms) and II are shown separately in (D).

Table I. Hyperfine Parameters of Oxidized Co–Fe Cluster at 4.2 K

	site I[a]	site II
A_x, MHz[b]	−35	+27
A_y, MHz	−38	+27
A_z, MHz	−31	+32
ΔE_Q, mm/s	+1.35	−1.1
η	0.4	0.4
δ, mm/s[c]	0.44	0.35

[a] Two equivalent Fe belong to site I. [b] Since $\bar{g}$ is quite isotropic, the labels x, y, and z have no spatial relation to the g_x, g_y, and g_z. See ref 8. [c] Isomer shifts are quoted relative to Fe metal at 298 K.

The lower trace in Figure 1A shows a 9 K EPR spectrum recorded under conditions where the signal of the Co–Fe cluster is partially saturated. The resonance at g = 2.01 belongs to unconverted Fe_3S_4 clusters.[1] Thus, the EPR spectra (as well as the Mössbauer spectra) allow us to estimate the conversion yield. For five preparations we determined that 55%, 73%, 85%, 89%, and 94% of the total Fe belonged to $CoFe_3S_4$ clusters, with the remainder in unconverted Fe_3S_4. Typically 60–70% of the starting material was recovered.

The Mössbauer spectra of two samples[6] are shown in Figure 2. At 183 K the spectra of the oxidized Co–Fe cluster (Figure 2B) consist of one slightly asymmetric doublet (suggesting inequivalent irons) with quadrupole splitting ΔE_Q = 1.10 mm/s and isomer shift δ = 0.36 mm/s. At 4.2 K the spectra exhibit paramagnetic hyperfine interactions. The response of the spectral intensities to weak applied fields[7] shows that the spectra result

(4) Moura, J. J. G.; Moura, I.; Kent, T. A.; Lipscomb, J. D.; Huynh, B. H.; LeGall, J.; Xavier, A. V.; Münck, E. *J. Biol. Chem.* **1982**, *257*, 6259–6267.
(5) Kent, T. A.; Dreyer, J.-L.; Kennedy, M. C.; Huynh, B. H.; Emptage, M. H.; Beinert, H.; Münck, E. *Proc. Natl. Acad. Sci. U.S.A.* **1982**, *79*, 1096–1100.
(6) The raw data contained contributions from unconverted 3Fe clusters. The sample of Figure 2A contained 6% of Fe_3S_4 according to EPR and an undetectable amount of Fe_3S_4 according to the Mössbauer data (the Mössbauer sample was quite dilute). Both techniques suggest 25–30% unconverted Fe_3S_4 for the sample of Figure 2B–D. For clarity we have subtracted the spectral contributions of Fe_3S_4 from the raw data to obtain the spectra of Figure 2B–D.
(7) Münck, E. *Methods Enzymol.* **1978**, *54*, 346–379.

from three iron atoms residing in the cluster which yields the observed EPR signal. Analyses of the 4.2 K spectra reveals two distinct sites with occupancy ratio of 2:1. We have described the data by the spin Hamiltonian ($S = {}^1/_2$)

$$\hat{H} = \beta\vec{S}\cdot\tilde{g}\cdot\vec{H} + \sum_{i=1}^{2}\{\vec{S}\cdot\tilde{A}(i)\cdot\vec{I}(i) - g_n\beta_n\vec{H}\cdot\vec{I}(i) + H_{quad}(i)\}$$

where i designates the two distinct sites. For details of such analyses see ref 8. The solid lines in Figure 2C,D are simulations using the parameters of Table I. The hyperfine tensors of the two types of Fe sites have different signs, an indication of a spin-coupled system.

Figure 2A shows a 4.2 K spectrum (ΔE_Q = 1.28 mm/s and δ = 0.53 mm/s) of a dithionite-reduced sample. In strong applied fields the spectra (not shown) exhibit magnetic hyperfine structure; i.e., the complex is paramagnetic with integer spin S.

The values for δ, which is a useful oxidation state marker, can be compared with those[4] of the Fe_4S_4 cluster produced by reconstitution of apo-Fd II. The average shift δ_{av} = 0.41 mm/s of the oxidized Co-Fe cluster compares well with δ_{av} = 0.44 mm/s of the $[Fe_4S_4]^{2+}$ cluster. Likewise, δ_{av} = 0.53 mm/s of the reduced Co-Fe cluster is very similar to δ_{av} = 0.57 mm/s observed[4] for $[Fe_4S_4]^{+}$. These observations, as well as the EPR results, suggest that a $[CoFe_3S_4]^{2+}$ cluster is isoelectronic with a $[Fe_4S_4]^{+}$ cluster.

In summary, the Mössbauer and EPR studies as well as chemical analysis suggest the presence of a novel cluster with a $CoFe_3S_4$ core. The formation of a $CoFe_3S_4$ cluster in Fd II shows that Fe_3S_4 clusters, incorporated into a protein matrix, can serve as promising precursors for the formation of novel clusters. We have preliminary evidence for the formation of a cluster containing copper.

Acknowledgment. We thank Dr. J. D. Lipscomb for making his EPR facility available and P. Kelly, N. Hart, and the staff of the University of Georgia Fermentation Plant for growing *D.gigas* cells. This work was supported by the National Science Foundation, the National Institutes of Health, the Instituto de Investigação Cientifica Tecnologica, the Junta Nacional de Investigação Cientifica Tecnologica, and the Agency for International Development.

(8) Christner, J. A.; Janick, P. A.; Siegel, L. M.; Münck, E. *J. Biol. Chem.* **1983**, *258*, 11157-11164.

Synthesis and X-ray Crystal Structure of the Stable Paramagnetic Dihydrido Complex $Ir(H)_2(Cl)_2(P\text{-}i\text{-}Pr_3)_2$[1]

Pasquale Mura

Istituto di Strutturistica Chimica "G.Giacomello"
Area della Ricerca di Roma, CNR
C.P. N. 10 00016 Monterotondo Stazione (RM), Italy

Received May 14, 1985

Paramagnetic transition-metal hydride complexes are very rare[2] and mainly characterized in solution.[3,4] To our knowledge only two complexes of tantalum[4] were stable enough in order to determine X-ray crystal structures.

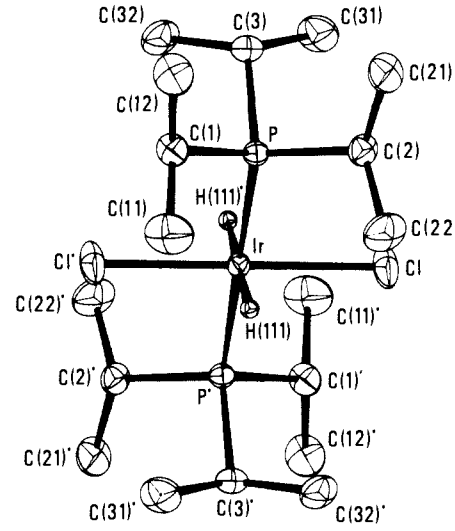

Figure 1. Geometry of the $Ir(H)_2(Cl)_2(P\text{-}i\text{-}Pr_3)_2$ molecule with hydrogen atoms of the P-*i*-Pr_3 groups omitted for clarity. The Ir atom occupies the position of crystallographic symmetry $\bar{1}$. Relevant bond distances (Å) and angles (deg): Ir-H(111) = Ir-H(111)', 1.90 (7); Ir-Cl = Ir-Cl', 2.342 (1); Ir-P = Ir-P', 2.360 (2); Cl-Ir-H(111) = Cl'-Ir-H(111)', 93 (2); P-Ir-H(111) = P'-Ir-H(111)', 70 (2); Cl-Ir-P = Cl'-Ir-P', 90.27 (4); H(111)-Ir-H(111)', 180.0; Cl-Ir-Cl', 180.0; P-Ir-P', 180.0.

Paramagnetic iridium(IV) complexes are stable and have been extensively investigated.[5] Furthermore iridium easily forms hydrido compounds in the formal oxidation states I, III, and V.[6,7]

We now report the first example of a paramagnetic hydrido complex of Ir, i.e., the octahedral compound $Ir^{IV}(H)_2(Cl)_2(P\text{-}i\text{-}Pr_3)_2$ (**1**), Figure 1. To our knowledge, no other stable paramagnetic hydrido complexes of platinum group metals have been reported in the literature.

Ammonium hexachloroiridate $[(NH_4)_2IrCl_6]$, when reacted with an excess of triisopropylphosphine in refluxing ethanol (containing concentrated HCl), gives **1** as deep-purple, air-stable microcrystals (yield 31% based on $(NH_4)_2IrCl_6$). Elemental analyses[8a] of monomeric[8b] **1** are consistent with the presence of two P-*i*-Pr_3 groups and two chlorine atoms. Its IR spectrum (KBr pellets) shows one band at 2003 cm^{-1} (m, w) attributed to ν(Ir-H).[9] In the far-IR spectrum **1** shows strong sharp band at 317 cm^{-1} indicating the presence of trans chlorine atoms.[10] The magnetic moment[11] of **1** at room temperature gives a value of 1.54 μ_B, in agreement with a spin-paired d^5 electron configuration (Ir(IV) low spin).[10,12] Thus **1** is a 17-electron hydride complex. For further experimental details see the supplementary material.

The geometry around the iridium atom is that of a slightly distorted octahedron, with three pairs of trans ligands P-*i*-Pr_3, Cl, and H.[13,14]

(1) Presented, in part, at the XIIth International Conference on Organometallic Chemistry, Vienna, Sept 8, 1985.

(2) (a) Rhodes, L. F.; Zubkowski, J. D.; Folting, K.; Huffman, J. C.; Caulton, K. G. *Inorg. Chem.* **1982**, *21*, 4185-4192 and references cited therein. (b) Rhodes, L. F.; Caulton, K. G. *J. Am. Chem. Soc.* **1985**, *107*, 259-260 and references cited therein.

(3) Allison, J. D.; Walton, R. A. *J. Am. Chem. Soc.* **1984**, *106*, 163-168 and references cited therein.

(4) Luetkens, M. L., Jr.; Elcesser, W. L.; Huffman, J. C.; Sattelberger, A. P. *Inorg. Chem.* **1984**, *23*, 1718-1726 and references cited therein.

(5) (a) Chatt, J.; Leigh, G. J.; Mingos, D. M. P.; Paske, R. J. *J. Chem. Soc. A* **1968**, 2636-2641 and references cited therein. (b) Fergusson, J. E.; Rankin, D. A. *Aust. J. Chem.* **1983**, *36*, 863-869 and references cited therein. (c) Rankin, D. A.; Penfold, B. R., Fergusson, J. E. *Ibid.* **1983**, *36*, 871-883 and references cited therein. (d) Isobe, K.; Vazquez de Miguel, A.; Nutton, A.; Maitlis, P. M. *J. Chem. Soc., Dalton Trans.* **1984**, 929-933 and references cited therein.

(6) For general reviews, see: (a) Muetterties, E. L., Ed. "Transition Metal Hydrides"; Marcel Dekker: New York, 1971. (b) Bau, R., Ed. *Adv. Chem. Ser.* **1978**, *No. 167*. (c) Teller, R. G.; Bau, R. *Struct. Bonding (Berlin)* **1981**, *44*, 1-82.

(7) Gomez, M.; Robinson, D. J.; Maitlis, P. M. *J. Chem. Soc., Chem. Commun.* **1983**, 825-826 and references cited therein.

(8) (a) Satisfactory elemental analyses were obtained; see supplementary material. (b) Satisfactory molecular weight was obtained; see supplementary material.

(9) Attempts to obtain **1**-d_2 led to extensive deuteration of the organic ligands, which overlapped with the Ir-D band.

(10) Bennet, M. A.; Milner, D. L. *J. Am. Chem. Soc.* **1969**, *91*, 6983-6994 and references cited therein.

(11) For magnetic measurements see supplementary material.

(12) Figgis, B. N. "Introduction to Ligand Fields"; Wiley: New York, 1966; pp 305-306.

0002-7863/86/1508-0351$01.50/0